Shapes of strongly absorbed polyelectrolytes in poor solvents

S. K. Pattanayek[1] and G. G. Pereira[2]
[1]*Department of Mechanical Engineering, University of Sydney, Sydney, Australia*
[2]*MacDiarmid Institute, School of Chemical and Physical Sciences, Victoria University of Wellington, Wellington, New Zealand*
(Received 6 November 2006; revised manuscript received 23 January 2007; published 15 May 2007)

The pearl necklace instability has been predicted to occur for single polyelectrolyte chains immersed in an incompatible (or poor) solvent, but still direct imaging of this chain conformation is not conclusive. We therefore examine how a surface may interact with the polyelectrolyte to, possibly, inhibit this instability. We show from explicit calculations that for strongly absorbed polyelectrolyte chains another conformation of the chain is stable in parts of the diagram of states. We support this calculation with more rigorous numerical, self-consistent mean field calculations which exhibit both elliptical globules and a pseudo pearl necklace structure.

DOI: 10.1103/PhysRevE.75.051802 PACS number(s): 82.35.Rs, 68.35.Md, 68.47.Mn

I. INTRODUCTION

Chain molecules which bear charged monomers, called polyelectrolytes, have widespread applications but only relatively recently have received serious attention. The shape (or conformation) of the polyelectrolyte chain is one of the most fundamental physical properties, since the polyelectrolyte's applicability stems directly from this conformation. One of the most dramatic manifestations of this is the pearl necklace instability predicted first by Kantor and Kardar [1] and elucidated by Dobrynin *et al.* [2]. Since the original prediction of this unusual shape there have been numerous experiments on verifying the model. In most cases results have to be related to competing models, i.e., an elongated cylindrical morphology (or cigar) or a pearl necklace structure and the validity of either model is then inferred from these comparisons [3]. Thus the results, themselves, do not unequivocally demonstrate a pearl necklace structure, but rather give further evidence to support the prediction. On the other hand, direct experimental observations such as with atomic force microscopy or surface force apparatus have been more inconclusive. Direct imaging of single polyelectrolyte chains, involve a surface which often absorbs the chain either partially or completely [4]. This implies surface phenomena are important in determining the final conformations of absorbed polyelectrolyte chains, which are imaged in these experiments. Therefore we address the following question in this study: Will a polyelectrolyte in a poor solvent, but strongly absorbed on a flat two-dimensional surface, still exhibit a Rayleigh-like instability? Furthermore, we investigate the possible shapes of the absorbed chain. The results presented here demonstrate that surfaces do indeed play an important role and can affect the pearl necklace morphology.

The bulk behavior of single polyelectrolyte chains in a poor solvent was originally studied by Khokhlov [5]. At low charge fraction, f, the globule takes on a spherical shape. Above a critical f, Khokhlov proposed the preferred shape of the charged globule should be an extended cylinder. However, subsequent work [1,2] showed such a conformation was unstable to capillary wave fluctuations and ultimately the globule deforms to a pearl necklace with two beads (called a dumbbell). For increasing f this dumbbell could further split into a necklace with three beads and so on. These shapes represent a delicate balance between the two major contributions to the globules free energy—the electrostatic repulsion between charged monomers, which promotes an extended conformation, and the surface tension between polymer and solvent which promotes collapse to a sphere. For direct imaging of such chains, the surface must absorb the chain so that there exists an overall preference of the polymer for the surface. The surface on which the polyelectrolyte is absorbed is assumed to be uncharged [6]. As a consequence of the charged globule in the vicinity of this surface, the Coulomb interaction will be modified from the bulk case. The presence of a dielectric boundary, being the x-y plane located at $z=0$, implies a discontinuity in the perpendicular component of the electric field [7]. The Coulomb interaction between a charge q_1 (which is at $\mathbf{r}$ and in the half-space $z \geqslant 0$) and a second charge q_2 (which is at $\mathbf{r}'$ also in the half-space $z \geqslant 0$) is then given by [8]

$$V(\mathbf{r},\mathbf{r}') = \frac{q_1 q_2}{\epsilon}\left[\frac{1}{|\mathbf{r}-\mathbf{r}'|} + \frac{(1-\epsilon'/\epsilon)}{(1+\epsilon'/\epsilon)}\frac{1}{\sqrt{(\mathbf{r}-\mathbf{r}')^2+4zz'}}\right]. \tag{1}$$

Our present problem now applies to two special limits of the above formula. First, the dielectric substrate has low dielectric constant in comparison to a typical solvent (for example, water). A typical value for the dielectric constant of water (with respect to a vacuum) is around 80, while that of mica (a typical AFM/SFA substrate) is around 5. Thus $\epsilon'/\epsilon \ll 1$. Secondly, we assume the monomers are on the surface of the dielectric surface so that $z=z'=0$. With these two assumptions the Coulomb interaction between two charges at $\mathbf{r}$ and $\mathbf{r}'$, such that the two charges have zero z component, is just

$$V(\mathbf{r},\mathbf{r}') = \frac{2q_1 q_2}{\epsilon|\mathbf{r}-\mathbf{r}'|}. \tag{2}$$

We therefore see that the 3D Coulomb interaction is modified by a multiplicative factor of 2, so that the functional dependence of the Couolmb potential is the same in 2D as in 3D. Also, as the polyelectrolyte nears the surface, charge will build up. Cohen-Stuart *et al.* [9] have considered this problem and showed this can lead to a kinetic slowing down of

polyelectrolyte absorption. For a few reasons this may not be important for the case studied here. First, the chains we consider have a low net charge and so charge build up at the surface will be small. Secondly, our globule is assumed to be spread rather thinly over the surface and due to the short range surface attraction there should still be a net gain in absorbing on the surface. Finally, since we are interested in equilibrium effects in this paper, the final absorbed state of the polyelectrolyte should not be affected by this (small) repulsive barrier.

Once the polyelectrolyte is strongly absorbed to the surface the important question is whether the isotropic shape of the globule (in this case either a circle or a spherical dome) is stable in comparison to the pearl necklace structure? If not, what new conformations of the chain are possible? As a clue to what may happen, we recall that although a stretched (neutral) polymer in a poor solvent is unstable to capillary wave fluctuations, i.e., the Rayleigh—Plateau instability [10] a strongly absorbed (neutral) polymer is not [11,12]. We use two independent methods to determine the shape of the charged globule—explicit comparison of the globule's free energy for a few different shapes and self-consistent mean field theory (SCF). Both methods agree on the final shapes.

Since we are interested in the poor solvent regime, below the Θ temperature of the chain, we define the reduced temperature, τ, where $\tau \equiv (\Theta - T)/\Theta$ and T is the actual temperature [2]. When a droplet of liquid absorbs onto a flat surface the contact angle, θ is given by a balance of three surface tensions—polymer-solvent γ_{PS}, polymer-surface, γ_{PF}, and the solvent-surface γ_{SF}. The contact angle then satisfies $\cos\theta = (\gamma_{SF} - \gamma_{PF})/\gamma_{PS}$. For a hydrophobic surface and hydrophobic polymer, which is the case we are interested in here, we have $\gamma_{SF} \approx \gamma_{PS} \gg \gamma_{PF}$. This implies the contact angle is $\cos\theta = 1 - \delta$, where $\delta \equiv \gamma_{PF}/\gamma_{PS} \ll 1$. We denote the number of monomers in the polymer chain by N and each monomer has size b. The droplet assumes the shape of the dome of a sphere of radius R and volume $V_D = \pi R^3[2 - 3\cos\theta + \cos^3\theta]/3$. At the reduced temperature, τ, the globular volume is Nb^3/τ, so that the radius of the sphere is fully determined in terms of N, τ, and θ. As the contact angle diminishes the droplet takes on a flatter aspect. This cannot continue indefinitely. There is an upper limit to the radius of the sphere. Beyond this limit the droplet adopts the shape of a flat layer or pancake of thickness h, equal to b/τ (i.e., the thermal blob size [2]), and radius $R_{\|} = (N/\pi)^{1/2} b$. At this stage the problem becomes two-dimensional. Thus we find there exists a critical N, denoted N_{crit}, below which the system is two-dimensional. This is given by $N_{crit} = 9\pi \sin^6\theta \tau^{-2}[2 - 3\cos\theta + \cos^3\theta]^{-2}$. For small θ, we find $N_{crit} \approx 63.6(\tau\theta)^{-2} = 31.8(\tau^2\delta)^{-1}$. If the surface tension ratio δ is even smaller, the thermal blob deforms in the direction perpendicular to the surface, i.e., the thickness of the pancake decreases from b/τ according to $h = \delta^{2/3}(N/\pi\tau)^{1/3} b$, until its minimum thickness of b. Thus the two-dimensional model is important for relatively strong absorption (i.e., δ small) and such globules have been observed experimentally [13]. Finally, there are other effects which may stabilize the thickness of the pancake such as thermal fluctuations or long range interactions, which are beyond the scope of this paper.

II. EXPLICIT FREE ENERGY

To begin we consider the stability of an elongated (ellipsoidal) globule in bulk solution. We shall see an ellipsoidal globule is stable, compared to a spherical globule, only for relatively large f and correspondingly large anisotropy of the globular shape. The argument given here is similar to that given by Kantor and Kardar [1], but we reproduce it here because it is not trivial and forms the basis for the absorbed globule analysis.

To consider the stability of an ellipsoidal globule in bulk (three-dimensions) solutions we determine the free energy of the droplet, as initially proposed by Kantor and Kardar [1] and Dobrynin *et al.* [2]. The two major contributions to the free energy of the condensed globule is a Coulomb (repulsive) energy and a surface energy. (In this case, entropic energy of the polymer chain can be shown to be negligible.) The Coulomb energy for any particular geometry is

$$F_{Coul} = \frac{k_B T l_B N^2 f^2}{V^2} \int_V \int_V \frac{1}{2|\mathbf{r} - \mathbf{r}'|} d\mathbf{r}\, d\mathbf{r}', \tag{3}$$

where $\mathbf{r}$ represents any point within the globule, f is the fraction of charged monomers, V represents the volume of the globule, and although the volume is constant the geometry can change. The extra factor of 2 accounts for double counting of pairs. The polyelectrolyte is considered uniformly charged, so that charge density is constant throughout the globule. With this assumption, the Coulomb energy may be written in terms of the Bjerrum length, defined as $l_B \equiv q^2/(\epsilon_p k_B T)$, where q is the electronic charge, ϵ_p the dielectric constant of the polymer and $k_B T$ is the thermal energy. For certain special cases the integrals in Eq. (3) can be evaluated exactly. For a sphere of radius R we obtain $3k_B T l_B f^2 N^2/(5R)$ and since the volume of a sphere is $V = 4\pi R^3/3$, the Coulomb energy of the sphere can be written as $F_{C0} = 3k_B T l_B f^2 N^2 (4\pi)^{1/3}/[5(3V)^{1/3}]$. On increasing charge fraction, the sphere would be expected to elongate into a prolate spheroid, with a long axis R and two shorter axes, each of the same length, c. The volume of the prolate spheroid is $V = 4\pi R^3(1 - e^2)/3$, where the eccentricity, e, is defined as $e^2 = 1 - c^2/R^2$. This volume is constant so that as e increases, R must also increase. The Coulomb energy of the prolate spheroid is

$$F_{Coul} = F_{C0}(1 - e^2)^{1/3} \frac{1}{2e} \ln\left[\frac{1 + e}{1 - e}\right]. \tag{4}$$

The surface energy of the droplet is just $F_{surf} = \gamma \mathcal{A}$, where γ is the surface tension and $\mathcal{A}$ is the surface area of the globule. Once again, for simple geometries this area is given precisely, i.e., for a sphere is $4\pi R^2$ and for a prolate spheroid is $2\pi R^2(1 - e^2)[1 + (1 - e^2)^{-1/2} e^{-1} \arcsin e]$. The surface energy of a spherical droplet can be written as $F_{S0} = 4\pi k_B T \sigma (3V/4\pi b^3)^{2/3}$, where $\sigma \equiv \gamma b^2/(k_B T)$. Thus the prolate spheroid's surface energy is

$$F_{surf} = F_{S0}(1 - e^2)^{1/3} \frac{1}{2}\left[1 + \frac{\arcsin e}{e\sqrt{1 - e^2}}\right], \tag{5}$$

while the total free energy of a prolate spheroid is

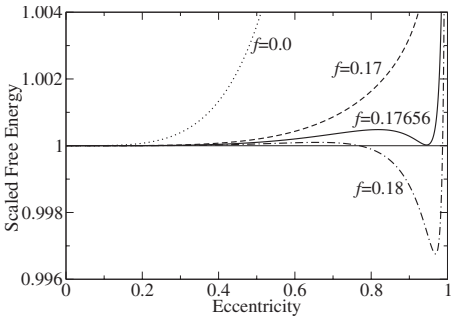

FIG. 1. Scaled free energy, F/F_{sphere}, of a bulk (three-dimensional) charged droplet of liquid (of either spherical geometry, $e=0$, or a prolate spheroid geometry, $e\neq 0$) in a poor solvent versus eccentricity of the droplet. For this plot we use $N=100$, $\sigma=1$, $u\equiv l_b/b=2$ and charge fractions of $f=0$ (dotted), $f=0.17$ (dashed), $f=f_{\text{crit}}\approx 0.17656$ (full), and $f=0.18$ (dot-dashed). Note that a prolate spheroid (with nonzero eccentricity) only becomes stable for relatively large f and at very large values of e, when the prolate spheroid would be almost cigarlike in shape.

$$F_{\text{prolate}}=\frac{(1-e^2)^{1/3}}{2}\left\{F_{S0}\left[1+\frac{\arcsin e}{e\sqrt{1-e^2}}\right]+\frac{F_{C0}}{e}\ln\left[\frac{1+e}{1-e}\right]\right\}. \tag{6}$$

Note that embedded in F_{C0} is f, the fraction of charged monomers along the chain. We now plot this free energy for $N=100$, $\sigma=1$, $u\equiv l_b/b=2$ and various values of f (Fig. 1), as a function of eccentricity, e. (In fact we scale the energy with respect to a spherical globule's energy, i.e., $F_{\text{sphere}}\equiv F_{S0}+F_{C0}$.) At small f we find the minimum is always at $e=0$. As f increases a secondary minimum develops in the free energy curve, at large e. Eventually at a critical charge fraction, f_{crit} this second minimum has an energy equal to the minimum at $e=0$. It is important to note, this occurs at very large eccentricity, which implies the globule will be highly extended, almost cigarlike in shape. In this case, $f_{\text{crit}}\approx 0.17656$ and the corresponding $e\approx 0.944$. Note, on increasing charge the shape of the globule would appear to change discontinuously from a sphere ($e=0$) to a highly eccentric prolate spheroid ($e=0.944$). These results are typical of the (bulk) three-dimensional case—the prolate spheroid globule becomes stable for sufficiently large f, but has an extreme eccentricity.

Clearly, before the prolate spheroid globule becomes stable, a dumbbell may have a lower free energy. A dumbbell consists of two (small) spheres, of radius r connected by a long, thin, cylindrical string of length L and radius b/τ [2]. This has been shown previously by Kantor and Kardar [1] and also Dobrynin *et al.* [2], so we refer the interested reader to these articles. As a result, in bulk solutions, the condensed globule either takes the shape of an (isotropic) sphere or a dumbbell, with spherical beads. As the charge of the polymer increases the dumbbell will deform to a three-bead necklace and so on. In summary, in bulk solutions, within the simplest model which only includes electrostatic and surface energy contributions, the (anisotropic) prolate spheroid morphology of a condensed globule is never stable.

A. Strongly absorbed condensates

For strongly absorbed polymer condensates, i.e., in two dimensions, this is not the case. Recall, from the Introduction, we are dealing with strongly absorbed globules which will be of constant thickness (a layer or pancake) on the flat surface. We now concentrate on the shape of the globule in the plane of the surface and calculate the free energy of three different globular shapes: (i) An isotropic (circular) shape, (ii) an elliptical shape, and (iii) a dumbbell. The advantage of the elliptical shape over a circular one is that by elongating the Coulomb repulsion energy reduces, which is important as f increases. On the other hand, the advantage of the elliptical globule over a dumbbell is that it has a lower surface energy. In contrast to three dimensions, we shall see an elliptical shape *is* stable in two dimensions.

To calculate the free energy of the two-dimensional structures we follow the same prescription as outlined above, for the ellipsoidal globule. However, the surface energy now corresponds to the perimeter length of the globule, since the upper surface area of the pancakelike globule is the same for all structures. Secondly, the Coulomb energy of the ellipse is no longer determined by an analytic expression but, rather, has to be calculated numerically. In addition, we calculate the Coulomb energy of the dumbbell numerically, rather than making any simplifying approximations. Consider first the elliptical pancake structure. The surface energy is just $F_{\text{surf}}=\gamma\mathcal{P}h$, where γ is the surface tension and $\mathcal{P}$ is the perimeter length of the globule. Note, one may argue here that the concept of a surface tension becomes debatable as the pancake's thickness becomes smaller and smaller. While this is strictly true, we take the view here that since all globules have the same thickness [set by $h=\delta^{2/3}(N/\pi\tau)^{1/3}b$] it is the perimeter length which is the important quantity. The perimeter length remains large (i.e., much larger than b) and so the concept of a surface tension is still valid. In truth, γ should then be referred to as a *line tension*, which is what Sevick and Williams [11] called it when studying strongly absorbed polymers on a flat surface. As described in the paper by Dobrynin *et al.* [2], we assume γ is k_BT per thermal blob so $\gamma\approx k_BT\tau^2/b^2$. The total free energy, F, is a sum of these two terms, i.e., $F=F_{\text{Coul}}+F_{\text{surf}}$. The elliptical pancake, of thickness h, has a semimajor axis l_x and semiminor axis l_y with eccentricity $e\equiv\sqrt{1-l_y^2/l_x^2}$. Volume conservation for this pancake implies $Nb^3/\tau=\pi l_x^2 h(1-e^2)^{1/2}$, which leaves one free variable. (Recall, h is determined by the surface tension ratio, δ.) Thus the surface energy of the ellipse is

$$F_{\text{surf}}=4k_BT\tau^2\frac{l_x}{b}\frac{h}{b}E(e), \tag{7}$$

where $E(e)$ is an elliptical integral of the second kind [14]. The Coulomb energy is calculated numerically for this geometry via Eq. (3). The free energy for the ellipse is therefore minimized over the free variable (let it be e) to find the optimally shaped elliptical globule.

The same method is used for the dumbbell structure, where the two variables are the string length L and the radius of the bead r (see Fig. 2). The width of a string is b/τ [2]. The volume constraint condition for the dumbbell case is

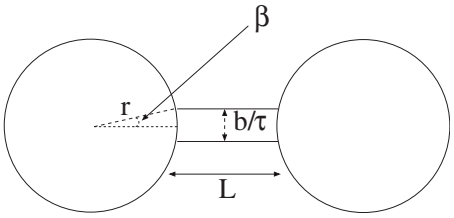

FIG. 2. Schematic of a dumbbell, with beads of radius r, connected by a string of length L and width b/τ. Angle β is defined in the text.

$$\frac{Nb^3}{\tau} = \left[2\pi r^2 + \frac{Lb}{\tau} - r^2(\beta - \sin\beta) \right] h, \tag{8}$$

where $\beta \equiv 2\arcsin([2\tau r/b]^{-1})$. The surface energy for the dumbbell is

$$F_{\text{surf}} = 2k_B T \tau^2 \left[(2\pi - \beta)\frac{r}{b} + \frac{L}{b} \right] \frac{h}{b}. \tag{9}$$

The Coulomb energy is calculated numerically via Eq. (3). Once again one variable is eliminated (let it be L) and the dumbbell energy is minimized over the remaining variable. The whole minimization procedure is computed numerically for each condensate shape.

We shall do calculations for similar parameters to Dobrynin *et al.* [2], i.e., $N=100$ and $u \equiv l_B/b=2$. It is important to realize that for strongly absorbed polymers (i.e., in 2D) the poor solvent regime exists at higher reduced temperature τ than for polymers in bulk solution (i.e., 3D). This was first discussed by Joanny [15]. Thus for certain values of τ, even though the polymer could be in the poor solvent regime in bulk solution, it may not be so for the strongly absorbed polymer. We therefore now determine the poor solvent regime for the 2D polymer. In two dimensions, a Θ polymer has average size $R_g \sim N^{\nu} b$, where $\nu=4/7$ [16], while in a poor solvent the size of the globule is $(N/\tau)^{1/2} b$. This implies the poor solvent regime exists for $\tau > N^{1-2\nu}$. For $N=100$ this implies $\tau > 0.51$. (Note, for these values of N and τ, the globule would be a pancake for $\delta < 1/2$.) We show typical free energy curves in this region, i.e., $\tau=0.6$ and $h=b$. We plot the dimensionless free energy $F/k_B T$ versus charge fraction, f for both the ellipse (bold line) and the dumbbell (dashed line); see Fig. 3. At zero charge the ellipse (in fact a circle) has the lowest energy. Eventually, on increasing charge there is a crossover in energies, until at higher charge fraction the dumbbell has lower energy. On the same graph (right-hand scale) we plot the square of the eccentricity (dot-dashed curve) as a function of f. In contrast to the three-dimensional case, the isotropic (circular) droplet deforms to an elliptical geometry with a gradually increasing eccentricity, i.e., the transition, from circle to ellipse, appears to be continuous. The eccentricity increases to $e^2 \approx 0.9$ (which corresponds to $l_x \approx 3 l_y$), just before the transition to the dumbbell state. Meanwhile, on increasing charge the circles, which make up the dumbbells, diminish in size since more polyelectrolyte is taken up by the strings. For larger δ (i.e., $h > b$) the same qualitative results are evident, although the eccentricity of the ellipse (before the transition to a dumbbell) in these cases is smaller. Such behavior is expected since, as the pancake thickness increases, one would expect to evolve closer to the three-dimensional (bulk solution) results.

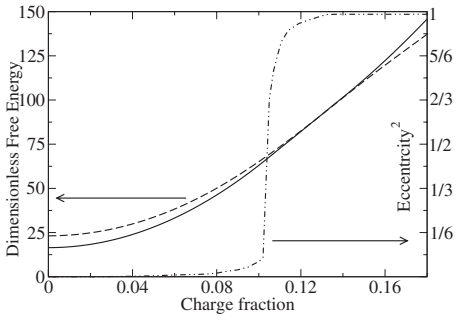

FIG. 3. Dimensionless free energy (left-hand scale), $F/k_B T$, versus charge fraction, f for ellipse (bold) and dumbbell (dashed) at a reduced temperature of $\tau=0.6$. The dot-dashed line is the square of the eccentricity of ellipse (right-hand scale). The crossover from ellipse to dumbbell occurs at $f \approx 0.125$ and the eccentricity of the ellipse at this point is $e^2 \approx 0.9$.

Next we discuss the shape of the actual beads which make up the pearl necklace. In three dimensions the beads of the necklace are always isotropic, i.e., spherical [1]. In two dimensions, we question whether this is still the case. That is, are the beads of the pearl necklace always circular? To understand what happens here we note that when a polymer gains a nonzero net charge it can begin to deform to an anisotropic shape, i.e., the ellipse, to accommodate the extra electrostatic repulsion. This means a globule with a (relatively) small charge relaxes to an ellipse and then, when the critical charge is exceeded, fissions to a dumbbell. Since each bead in the necklace is then below the critical limit to fission, the shape of each individual bead is not always perfectly circular but, rather, can also be of an elliptical shape. This effect is shown quite dramatically in our numerical calculations (see Figs. 4–6). Therefore we predict that the beads, which form the pearl necklace, can also have an elliptical shape.

III. SELF-CONSISTENT FIELD METHOD

We now proceed to another method to analyze the shape of these strongly absorbed polyelectrolyte chains. The importance of implementing such a method is the following. We have so far assumed certain geometries for the polyelectrolyte chain, viz. ellipse and dumbbell, and shown that the ellipse is stable in certain parts of the diagram of states. However, we have *imposed* these geometries—we would really like to now implement techniques which do *not* assume any particular geometrical bias. We simply input the important molecular parameters and the particular (minimum free energy) structure should evolve from the calculation. The SCF method [17–19] is ideal for this and, as we shall see, yields detailed information on the globular shape. This is a *real-space* SCF technique which, for our present purposes of identifying unknown morphological structures, is much preferred to a basis-function method. Although the basis-

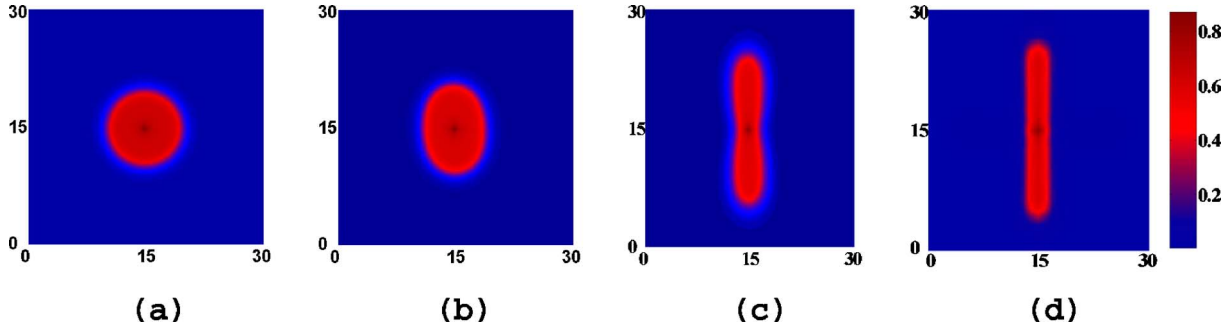

FIG. 4. (Color online) SCF results for $N=50$, $\chi=1$, $u=2$, $\epsilon_s/\epsilon_p=1.5$ and values of α (from left to right) (a) $\alpha=0.0$, (b) 0.163, (c) 0.17, and (d) 0.23. On increasing charge fraction we see a circular globule, then an elliptical globule, a "figure-8" and finally a strip. The scale bar on the extreme right gives the density to shading equivalence and the length scale is in units of b.

function method may give information on the absolute stability of a particular structure compared with another one, it is not useful when searching for unknown structures. In addition, we do not assume the dielectric constant is the same in polymer and solvent phases. Rather, these two phases have different dielectric constants and the overall dielectric constant at any point is dependent on the density of the phase at the particular point in space.

In the SCF method the important quantity is the probability distribution function, $q_p(\mathbf{r},t)$ for a chain of N monomers in total and whose tth monomer is at $\mathbf{r}$. (The variable t varies from 0 to N.) It can be shown this function satisfies the modified diffusion equation

$$\frac{\partial q_p(\mathbf{r},t)}{\partial t} = \frac{b^2}{6}\nabla^2 q_p(\mathbf{r},t) - [w_p(\mathbf{r}) + \alpha v_p \Psi(\mathbf{r})]q_p(\mathbf{r},t), \tag{10}$$

with initial condition $q_p(\mathbf{r},0)=1$. In the above equation the (pseudoexternal) mean field is denoted by $w_p(\mathbf{r})$ and is made up of short-range interactions between particles in the system [18]. Ψ is the (dimensionless) electric potential, i.e., $\Psi = q\psi/k_BT$, where q is the electronic charge, and can be determined via the Poisson equation. The Poisson equation involves the dielectric constant ϵ, which in principle varies, depending on the density of polymer or solvent present at the particular point in space. Thus we consider a dielectric constant, $\epsilon(\mathbf{r})$, which is a function of position, since we assume a strong segregation between polymer and solvent. We also measure this dielectric constant with respect to a pure polymer phase, so that $\epsilon(\mathbf{r})$ is dimensionless (see below for exact definition). We shall assume monomers are positively charged on dissociation. Thus for a position dependent ϵ, the Poisson equation becomes

$$b^2[\epsilon(\mathbf{r})\nabla^2\Psi(\mathbf{r}) + \nabla\epsilon(\mathbf{r})\cdot\nabla\Psi(\mathbf{r})] = -\frac{l_B}{b}[\alpha v_p \phi_p(\mathbf{r}) + v_-\phi_-], \tag{11}$$

where α is the degree of dissociation of monomer unit of the polymer, while v_p is the valency of charged monomers and v_- the valency of counterions. In Eq. (11), ϕ_p is the dimensionless polymer (probability) density, ϕ_s the dimensionless solvent (probability) density, and ϕ_- the dimensionless counterion (probability) density. For simplicity, we shall assume the positional dependent dielectric constant depends linearly on the density of the phase present at the particular point in space, i.e.,

$$\epsilon(\mathbf{r}) = \phi_p(\mathbf{r}) + \frac{\epsilon_s}{\epsilon_p}\phi_s(\mathbf{r}). \tag{12}$$

Note the dielectric constant, as defined above, is relative to a pure polymeric phase. In this case $\epsilon=1$. Equations (10)–(12) represent a coupled set of nonlinear partial differential equations, which need to be solved numerically. To close the system we require relationships between the probability dis-

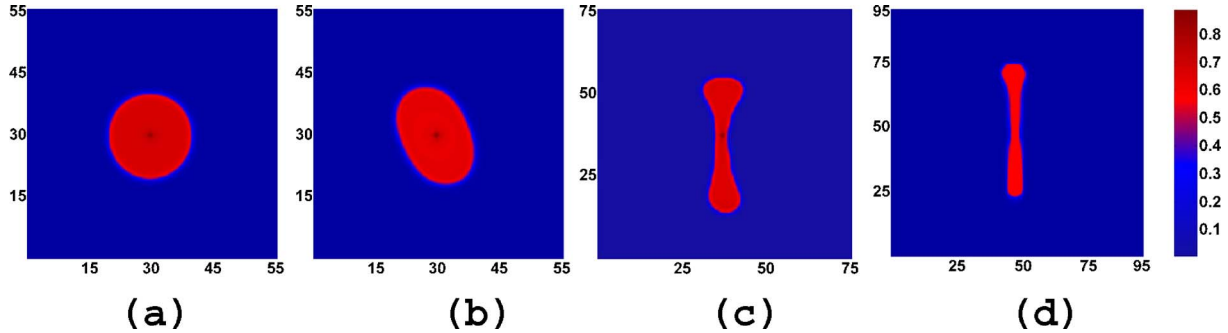

FIG. 5. (Color online) SCF results for $N=200$, $\chi=1$ and values of α (from left to right) (a) $\alpha=0.001$, (b) 0.0525, (c) 0.068, and (d) 0.09. On increasing charge fraction we see a circular globule, then an elliptical globule, a dumbbell, and finally a strip. The scale bar on the extreme right gives the density to shading equivalence and the length scale is in units of b.

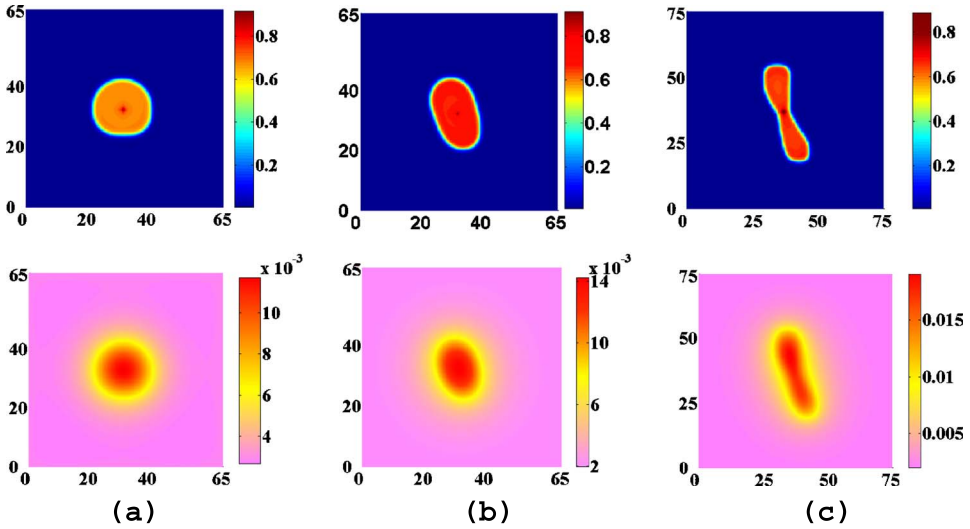

FIG. 6. (Color online) Polymer density (top) and counterion density (bottom) in the case where counterions are confined in the vicinity of condensate. SCF results for $N=200$, $\chi=1$, $u=2$, $\epsilon_s/\epsilon_p=1.5$ and values of α (from left to right) (a) $\alpha=0.0525$, (b) 0.065, and (c) 0.1. On increasing charge fraction we see a circular globule, then an elliptical globule, and finally a "figure-8" or dumbbell. The scale bar on the right-hand side gives the density to shading equivalence and the length scale is in units of b.

tribution functions and the polymer density, ϕ_p, and counterion density, ϕ_-, at any point $\mathbf{r}$. In principle one would like to have an infinite three-dimensional system with the polymer chain free to move on the two-dimensional surface plane and counterions free to move in all space. However, this is not possible at present due to computational limitations. To proceed we make some approximations. First, we graft one end of the polymer chain to the center of the square lattice, which represents the surface. This does not affect any of the physics we are interested in, but importantly prevents the polymer from moving beyond the boundaries. In addition we have to limit ourselves to a two-dimensional grid, which represents the surface. The probability distribution function for the chain starting from the grafted end, which is located at $\mathbf{r}_0$, is denoted by $Q_p(\mathbf{r},\mathbf{r}_0,t)$ and satisfies the modified diffusion equation

$$\frac{\partial Q_p(\mathbf{r},\mathbf{r}_0,t)}{\partial t} = \frac{b^2}{6}\nabla^2 Q_p(\mathbf{r},\mathbf{r}_0,t) - [w_p(\mathbf{r}) + \alpha v_p \Psi(\mathbf{r})]Q_p(\mathbf{r},\mathbf{r}_0,t), \quad (13)$$

with initial condition $Q_p(\mathbf{r},\mathbf{r}_0,0)=\delta(\mathbf{r}-\mathbf{r}_0)$. The polymer density at any point $\mathbf{r}$ is then given by

$$\phi_p(\mathbf{r}) = \frac{\int_0^N dt Q_p(\mathbf{r},\mathbf{r}_0,t) q_p(\mathbf{r},N-t)}{A^{-1}\int_A d\mathbf{r}\, Q_p(\mathbf{r},\mathbf{r}_0,N)}. \quad (14)$$

The extra factor in the denominator is introduced to normalize the density appropriately and A represents the total area of the square domain. The solvent density is determined via the volume constraint $\phi_p(\mathbf{r})+\phi_s(\mathbf{r})=1$, while the counterion density is given by

$$\phi_-(\mathbf{r}) = \frac{\exp[-w_-(\mathbf{r})]}{A^{-1}\int_A \exp[-w_-(\mathbf{r})]d\mathbf{r}}. \quad (15)$$

Last, the mean fields for the polymer and counterions are given by

$$w_p(\mathbf{r}) = \chi(1-2\phi_p(\mathbf{r})) - \ln(1-\phi_p(\mathbf{r}))$$

and

$$w_-(\mathbf{r}) = v_-\Psi(\mathbf{r}), \quad (16)$$

where χ, the Flory-Huggins parameter, measures the degree of incompatibility between polymer and solvent. Equations (10)–(16) are appropriately discretized on a two-dimensional grid and we begin our numerical relaxation procedure from a random (high temperature) state [12,17], which ensures no bias in the initial state. The boundary condition on the electric potential is obtained via Gauss' Law, i.e.,

$$[\epsilon(\nabla\Psi)_\perp]_{\text{boundary}} = -u\frac{\int_A [\alpha v_p \phi_p(\mathbf{r}) + v_-\phi_-(\mathbf{r})]d\mathbf{r}}{\mathcal{P}b^2}, \quad (17)$$

where the $\perp$ subscript indicates a normal component of the gradient of Ψ and the left-hand side is evaluated on the boundary of the grid. $\mathcal{P}$ is the perimeter length of the boundary, measured in units of b. The boundary condition on the probability distribution functions (q and Q) is that the normal component of their spatial gradient is zero. The numerical equations are iterated until we achieve self-consistency between the densities, the mean field and electrostatic potential. In principle, at this point, the system has evolved to a minimum free energy structure. (Note, we have used a criterion of a relative error of 10^{-6} for self-consistency.)

A. SCF results

We first assume the counterions are free in solution. For relatively low charge fraction this approximation is justified,

although later we will include the presence of counterions. Thus ϕ_- is set to zero in Eq. (11). We first consider $N=50$, $\chi=1$, $u=2$, $\epsilon_s/\epsilon_p=1.5$, $v_p=+1$, and increase α from $\alpha=0.0$ to 0.23. The sequence of results are shown in Fig. 4. The first case $\alpha=0$, results in a circular droplet. This shape persists until about $\alpha=0.16$ at which point the droplet takes on a much more elongated or elliptical shape. In fact, a closer examination of this transition reveals a rather gradual increase in the eccentricity of the ellipse. Figure 4(b) shows the globule at $\alpha=0.163$ where the ellipse has eccentricity of approximately 0.8, which corresponds to $l_x \approx 1.7 l_y$. At $\alpha=0.17$ [Fig. 4(c)], the globule appears to split into two droplets or beads, although the shape is more indicative of a sinusoidal undulation or a "figure-8" rather than a dumbbell. The strings seems to be missing here and is attributable to the small N for this chain. At the center of the figure-8 the width of the droplet is about $3.5b$, while at the widest part it is $4.6b$. Another important aspect of this structure is that the beads themselves are not circular but more elongated or elliptical, as the explicit free energy analysis suggests. At still higher α [Fig. 4(d)], we see a uniform elongation of the polymer globule into something which resembles a cigar, or in two dimensions a better description is a strip. At these low values of N we never see a complete dumbbell form, since the chain is too short to do this.

We therefore proceed to longer chains, i.e., $N=200$, with $\chi=1$, $u=2$, $\epsilon_s/\epsilon_p=1.5$, $v_p=+1$ and increasing α from $\alpha=0.0$ to $\alpha=0.09$. A typical sequence of results is shown in Fig. 5. The first case, $\alpha=0.001$, results in a circular globule. This shape persists until about $\alpha=0.045$ at which point the droplet takes on a more elongated shape. We have not investigated this circular to elliptical transition in detail, but our results (including many other runs) seem to indicate it is a continuous change. Figure 5(b) shows the density profile for $\alpha=0.0525$, where we see an anisotropic (elliptic) condensate. The eccentricity of this droplet is calculated to be approximately 0.75, which corresponds to $l_x \approx 1.5 l_y$. The elliptical globule remains until $\alpha=0.053$, at which point the globule takes on an elongated, "figure-8" shape. The string in this case is not clearly defined. [Figure is not shown but is similar to Fig. 4(c).] As we increase α to $\alpha=0.068$ the globule takes on the shape of a dumbbell. This is shown in Fig. 5(c), where the string is relatively thick. The beads of the dumbbell are not elongated, but somewhat circular. For higher values of α these beads do become elliptical themselves, in accordance with our earlier predictions, from the free energy analysis. At still higher α ($\alpha=0.09$) we see an almost uniform elongation of the droplet to a strip [Fig. 5(d)]. Here the remnants of the elliptical beads are just visible, if one looks closely at the two ends of the structure. At these relatively low values of N we never see more than two beads in the pearl necklace. Clearly, the chain is too short for it to form more than two beads. Although our SCF free energy minimization process does not ensure with absolute certainty that the structures in Figs. 4 and 5 correspond to the minimum free energy states, after several reruns from different initial conditions, we have always found the sequence in Figs. 4 and 5. Thus with high probability we believe the structures shown in Figs. 4 and 5 are the minimum free energy states.

Next we consider the role of counterions. At this stage, due to computational limitations, we cannot extend our simulations to a full three-dimensional lattice. [For example, Fig. 5(a) would take up to a month to run in three dimensions.] As a result, we cannot rigorously determine the behavior of the system when counterions are present. However, it is well known at sufficiently high charge fraction (or sufficiently poor solvent conditions) counterions will condense on the charged globule [2,20]. There are a number of possible effects which may now come into play. For example, the counterions can now screen the long range Coulomb repulsion and effectively renormalize the length scale of this repulsion. In turn, this stabilizes larger beads (or conversely the elliptical condensate) and, overall, the condensate dimensions should shrink. Hence, we (qualitatively) predict that the transitions (from circular to elliptical condensate and so on) should increase with α in the presence of condensed counterions, i.e., the charge fraction for the transition from an elliptical globule to a dumbbell should increase in comparison to the case where counterions do not condense on the globule. Although we cannot fully determine the role of counterions, we now consider the case where counterions are fully confined to the two-dimensional plane of the surface *and* in the vicinity of the condensate. The counterions could therefore be considered to have condensed on the globule.

Figure 6 shows a set of plots for the case where counterions are included in our SCF model, with ϕ_- nonzero in Eq. (11) and $v_-=-v_p$. All other parameters are the same as for Fig. 5. The main difference, compared with Fig. 5, is that the values of α where the circle, ellipse, and dumbbell are stable are slightly increased. Note, we have not observed a uniformly elongated cigarlike structure. Presumably this is because the counterions screen the long-range Coulomb repulsion, which in turn stabilizes smaller, more compact, morphological structures. We also plot the counterion density, but note that the density scale is significantly smaller (between 100–1000 times smaller) than the polymer density. In each case the counterion density closely follows the polymer density profile. Thus the main qualitative difference in having counterions present (so that they can condense on the polymer globule) is to increase the α transition values. Our results follow a similar pattern to discussed above, i.e., circle $\rightarrow$ ellipse $\rightarrow$ dumbbell, except now the transitions are shifted to higher α. For example, we now observe the figure-8/dumbbell structure at $\alpha=0.1$, whereas without counterions this structure appeared at $\alpha=0.053$. Although our assumption on counterion confinement is unrealistic at these low charge fractions, our results demonstrate counterions stabilize more compact structures such as the elliptical condensate in comparison to the more elongated (dumbbell) structure.

IV. CONCLUSIONS

In this paper, we have considered the shapes of strongly absorbed charged polymer globules in poor solvents, which has direct relevance to the imaging of such chains via AFM or SFA techniques [4,13]. We have shown that strongly absorbed polyelectrolytes have a different shape (or conformation) to polyelectrolytes in bulk solution. First, under sufficiently large absorption between the surface and polymer, the condensate will take up a layerlike (constant thickness) mor-

phology. Most notably we have predicted a new shape of the absorbed condensate (in the plane of the surface): An *elliptical* globule. Both our explicit free energy analysis and the numerical SCF calculations, which should evolve without any initial bias to the lowest free energy state, agree qualitatively on this prediction. However, the explicit calculations predict a larger distortion of the elliptical condensate (up to a semi-major axis three times the length of the semiminor axis) than the SCF calculations (which have shown a distortion of semimajor axis about 1.7 times the semiminor axis). The discrepancy between the size of the distortion is not unexpected, given the explicit model does not include entropy of chains which, if included, would tend to make the condensates less anisotropic (i.e., see Ref. [12]). In addition, we predict the beads which make up the pearl necklace may also be anisotropic. Our explicit free energy calculations imply the beads of the necklace may have an elliptical shape and the SCF results [for example, see Figs. 4(c), 5(d), and 6(c)] sometimes form a dumbbell where the beads have an elongated or elliptical shape. Finally we considered the presence of condensed counterions which tend to screen the long-range Coulomb interaction. In turn this stabilizes (more) compact elliptical morphologies in comparison to the (extended) dumbbell.

[1] Y. Kantor and M. Kardar, Phys. Rev. E **51**, 1299 (1995).
[2] A. V. Dobrynin, M. Rubinstein, and S. P. Obukhov, Macromolecules **29**, 2974 (1996).
[3] F. Bordi, C. Cametti, T. Gili, S. Sennato, S. Zuzzi, Z. Dou, and R. H. Colby, J. Chem. Phys. **122**, 234906 (2005).
[4] S. Minko, A. Kiriy, G. Gordodyska, and M. Stamm, J. Am. Chem. Soc. **124**, 3218 (2002); D. Baigl, M. Sferrazza, and C. E. Williams, Europhys. Lett. **62**, 110 (2003).
[5] A. R. Khokhlov, J. Phys. A **13**, 979 (1980).
[6] O. V. Borisov, F. Hakem, T. A. Vilgis, J.-F Joanny, and A. Johner, Eur. Phys. J. E **6**, 37 (2001).
[7] J. D. Jackson, *Classical Electrodynamics*, 3rd ed. (John Wiley & Sons, New York, 1999).
[8] R. Netz and J. F. Joanny, Macromolecules **32**, 9013 (1999).
[9] M. A. Cohen-Stuart, C. W. Hoogendam, and A. de Keizer, J. Phys.: Condens. Matter **9**, 7767 (1997).
[10] A. Halperin and E. Zhulina, Europhys. Lett. **15**, 417 (1991).
[11] E. M. Sevick and D. R. M. Williams, Phys. Rev. Lett. **82**, 2701 (1999).
[12] S. K. Pattanayek and G. G. Pereira, Macromol. Theory Simul. **14**, 347 (2005).
[13] S. A. Sukhishvili, Y. Chen, J. D. Muller, E. Gratton, K. S. Schweizer, and S. Granick, Nature (London) **406**, 146 (2000); M. S. Bakshi and S. Kaur, Colloid Polym. Sci. **284**, 74 (2005).
[14] M. Abramowitz and I. Stegun, *Handbook of Mathematical Functions* (Dover Publications, New York, 1970).
[15] J. F. Joanny, J. Phys. II **1**, 181 (1991).
[16] B. Duplantier and H. Saleur, Phys. Rev. Lett. **59**, 539 (1987).
[17] G. H. Fredrickson, V. Ganesan, and F. Drolet, Macromolecules **35**, 16 (2002).
[18] Q. Wang, T. Taniguchi, and G. H. Fredrickson, J. Phys. Chem. B **108**, 6733 (2004).
[19] A. C. Shi and J. Noolandi, Macromol. Theory Simul. **8**, 214 (1999).
[20] Q. Liao, A. V. Dobrynin, and M. Rubinstein, Macromolecules **39**, 1920 (2006).